日本医放会誌：52（8），1177—1182，1992（平4）

Digital Imaging of Dose Distributions using NMR Imager

Takeshi Hiraoka[1], Nobuo Fukuda[2], Hiroo Ikehira[2], Kazuo Hoshino[1], Yukio Tateno[2] and Katsuhiro Kawashima[1]

[1]Division of Physics and [2]Division of Clinical Research, National Institute of Radiological Sciences

Research Code No. : 203.2

Key Words : Dose distribution, Gel phantom, Digital image, MR imaging

核磁気共鳴映像法による線量分布の画像化

放射線医学総合研究所 [1]物理研究部 [2]臨床研究部

平岡　武[1]　福田　信男[2]　池平　博夫[2]

星野　一雄[1]　舘野　之男[2]　川島　勝弘[1]

（平成3年10月4日受付）

（平成3年11月25日最終原稿受付）

MRIとファントムを用いることにより，三次元の線量分布を画像としてとらえる方法といくつかの測定結果について報告する．Fricke溶液を放射線検出媒質とし，架橋デキストランゲル（Sephadex G-200）により溶液をゲル化して溶質の空間的移動を固定した．MRIによるプロトンの核スピン緩和率は照射した線量が25Gyまで比例関係が得られた．光子や電子線照射による線量分布画像の結果と，特に頭部や胸部ファントムによる画像結果について述べる．これらの方法は複雑な三次元治療計画への応用が期待される．

Introduction

In radiotherapy treatment planning for complex irradiation fields, it is necessary to obtain spatial dose distributions in patients. Gore et al[1] proposed a method for determining the spatial dose distributions in a tissue-equivalent phantom using nuclear magnetic resonance. Independent of their work, we started a study of this method[2], and present here the results. We describe various problems in making the gel phantom and give details of the images of dose distributions in some homogeneous and inhomogeneous phantoms.

Materials and Methods

A method for determining the spatial dose distribution in a tissue-equivalent phantom using nuclear magnetic resonance was proposed[2]. The concept involves irradiating an absorbing medium in which nuclear magnetic resonance properties change as a result of the interaction with ionizing radiation. A ferrous sulphate solution(Fricke solution[3]) in a gel is used as the detecting medium. A cross-linked dextran gel (Sephadex G-200) was used for this purpose.

When a dilute solution of ferrous sulfate in aerated sulfuric acid is irradiated, ferrous ions are converted into ferric ions in amounts proportional to the absorbed dose. The chemical reactions are

described by the following equations:

$$Fe^{++} + OH \rightarrow Fe^{+++} + OH^-$$
$$H + O_2 \rightarrow HO_2$$
$$Fe^{++} + HO_2 \rightarrow Fe^{+++} + HO_2^-$$
$$HO_2^- + H^+ \rightarrow H_2O_2$$
$$Fe^{++} + H_2O_2 \rightarrow Fe^{+++} + OH + OH^-$$

It has been observed that the change from Fe^{++} to Fe^{+++} reduces the relaxation time of the NMR of the protons surrounding the ion. Therefore, the longitudinal relaxation rate was observed by the alternating saturation recovery-inversion recovery sequence on a resistive type NMR imager (Asahi Mark-J, Asahi Medical Co., Japan) at 0.1 T. The longitudinal relaxation rate T_1 is given by[4]

$$T_1 = T_1(TI,TR) = \frac{TI}{\ln \frac{2SR(TR)}{D(TI,TR)}} \quad (1)$$

$$D(TI,TR) = SR(TR) - IR(TI,TR) \quad (2)$$
$$= 2\exp\left(-\frac{TI}{T_1}\right)$$

where TI (300 ms) is the inversion time, TR (20000 ms) the repetition time, SR the signal intensity of the saturation recovery image, and D(TI, TR) the signal intensity of the subtraction image, obtained by subtracting the inversion recovery (IR) image from the saturation recovery (SR) image. On the calculations, the influence of T_2 relaxation is ignored. To measure a dose distribution, the gel was made in the phantom which was then irradiated. The phantom then was moved into the NMR instrument, and T_1 was measured as a function of spatial distribution and then related to dose D with Eq(2).

Results

Several gels with varying compositions (for example, the concentration of $FeSO_4$, H_2SO_4 and NaCl; amount of Sephadex added to the solution; purity of H_2O) were prepared and used in preliminary experiments to determine the relationship between dose and relaxation time. In order to check the linearity and the repeatability of the relaxation rate as a function of absorbed dose, the irradiations were carried out on five separate days. Test tube with a 12 mm outer diameter, which were contained both the Fricke and the gel solutions, were irradiated by 12 MeV electron beams at the depth of peak absorbed dose. In Fig. 1, these functions of mentioned above are chosen for the Fricke solution and for the best combination found (containing 3.3% Sephadex G-200 by weight). The relaxation rate $R=1/T_1$ is shown as a function of dose D.

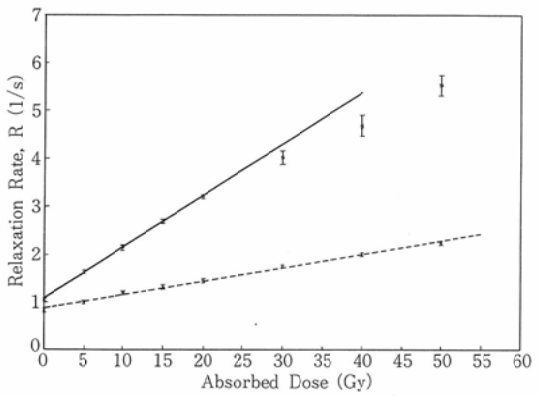

Fig. 1 Relaxation rate $R=1/T_1$ as a function of absorbed dose D for Fricke solution (dotted line) and the gel (solid line).

It is seen that the relationship between R and D is linear for a limited dose range. For the Fricke solution, the relation is R=0.8825 + (0.0279 ± 0.0009)D, for the gel it is R=1.094 + (0.1071 ± 0.0021)D. The latter gradient value is approximately four times larger than that of the Fricke solution. By varying the amount of Sephadex between 2% and 4%, the gradient of the relaxation rate changed by a maximum of 4%. This means that a small nonuniformity in the gel phantom does not influence dose distributions significantly. While it is necessary to use very pure distilled water to make the Fricke solutions, it is sufficient to use ordinary distilled water for the gel phantom.

Measurements of dose distribution with this method were made for several phantoms. Results are shown next. Fig. 2 shows an image of the dose distribution to the incident 15 MeV electron beams with a 10 cm × 10 cm field on the gel phantom. Irradiation was carried out by 30 Gy at the peak depth. As seen in the figure, we obtained smooth profile curves and a detailed image. The NMR measurement was made 30 minutes after irradiation. In Fig. 3 the lateral profiles in depth measured every 6 mm are shown, using the image of Fig. 2. The beam broadening with depth is seen clearly.

It is necessary to determine the degree of blurring of the image caused by diffusion of ferric ion in the gel phantom. As image of the gel phantom in Fig. 2 measured 21 hours after irradiation is shown in Fig. 4. The effect of diffusion is seen clearly in the lateral profile. At the 80% dose level the change in the width of the profile is 6 mm. After six hours, though, this change was only 1 mm.

The method works well for inhomogeneous phantom. Examples are shown next. Fig. 5 shows an image of a gel phantom in which lung (at left hand side, density ρ=0.3 g/cm^3) and bone (at right hand side, ρ=1.85 g/cm^3) substitutes[5] were introduced. The size of both substitutes was 2 cm wide and 2.5 cm deep. The full image, and lateral and depth dose profiles obtained with 15 MeV electron beams on a certain plane are shown. Details of the dose distributions are seen as an increase in dose near the bone by excess scattering of electrons from the bone. On the other hand, to the side of the lung, dose is decreased by fewer electrons scattered from the lung. In Fig. 6a an image is shown for an inhomogeneous gel phantom with lung and bone substitutes 5 cm wide and 2 cm deep. Schematic presentation of the irradiation is shown in Fig. 6b. The irradiation was carried out using 10 MV X-rays with a dose of 30 Gy at the peak depth.

Measurements were also made for sectional body phantoms. Fig. 7 shows a head phantom containing a human skull. The phantom surface was made of 2 mm thick polyester. Three liters of the gel were needed to fill up the phantom. Fig. 8 shows a thorax phantom containing human spine, cartilage and lung substitute. The phantom surface was made of 5 mm thick Lucite and lung substitute was made of a substance with density, ρ=0.3 g/cm^3. These phantoms were made by Kyoto Scientific Co. Ltd. Japan

Fig. 9 shows an image of the dose distribution in the head phantom obtained in a plane perpendicular to the beam axis for a 15 MeV electron beam with a field of 6 cm × 8 cm. In the dose distribution, the irregularities caused by the presence of skull and surface structures are clearly seen. An image of the head phantom in the coronal plane is shown in Fig. 10. No. MNR signals were obtained for the skull.

In general, lungs are one of the most frequently irradiated tissues in radiotherapy. Fig. 11 shows an image of four oblique fields simulated for treatment of the esophagus using the thorax phantom. Irradiations were carried out using 10 MV X-rays with an equal dose of 15 Gy at the peak depth for each field. Field sizes were 10 cm × 6 cm and no compensating filters were used. We see a good dose distribution in the target volume.

Discussion

We present a method for determining the dose distribution in a tussue-equivalent phantom using nuclear magnetic resonance. Measurement of three-dimensional dose distributions is possible, and is especially useful for radiation treatment planning for complex irradiation fields with inhomogeneous media. The method thus is useful for the production of dose distribution images needed in treatment

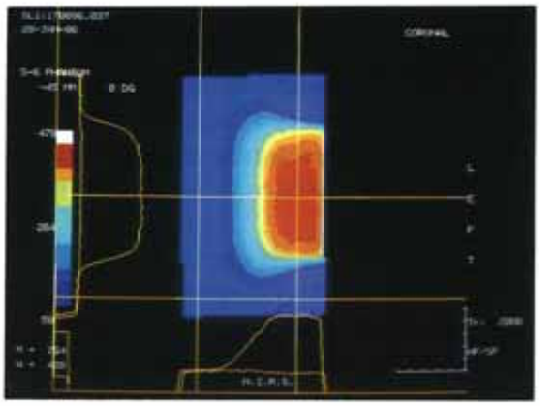

Fig. 2 Image of dose distribution of a 15 MeV electron beam incident on a homogeneous phantom. Lateral and depth dose profiles are shown with background level.

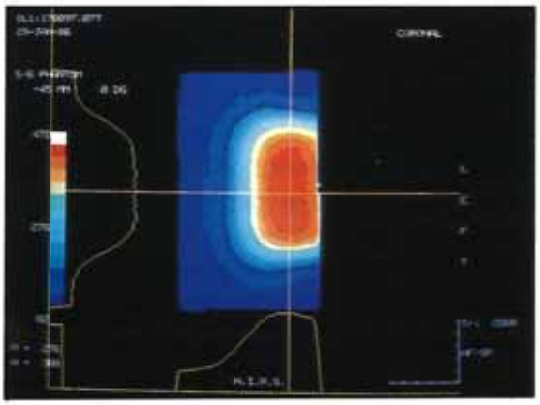

Fig. 4 NMR T_1 dependent images measured at 21 hours after irradiation.

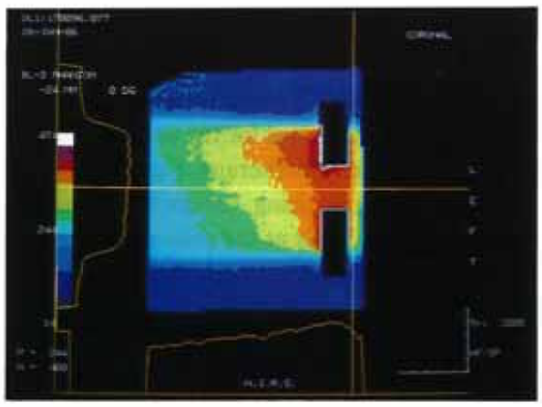

Fig. 6a Image in the incident 10 MV X-rays in the inhomogeneous phantom.

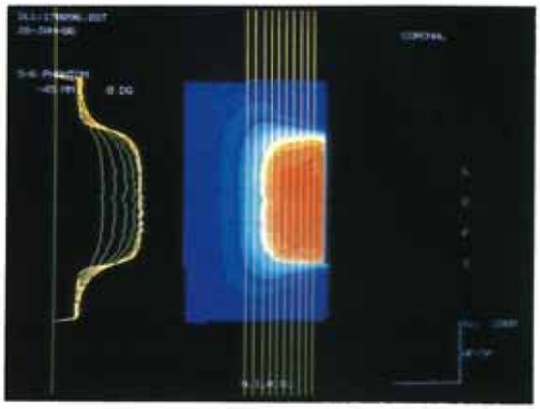

Fig. 3 Lateral profiles measured at several depths.

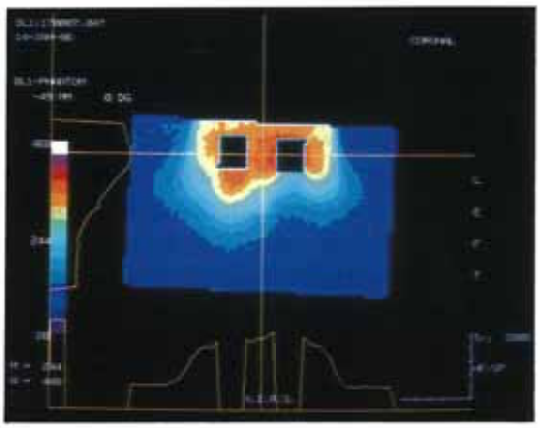

Fig. 5 Image in the gel phantom containing lung (left hand side) and bone (right hand side) substitutes irradiated with 15 MeV electrons. At present, dose inside lung and bone must be determined using other methods.

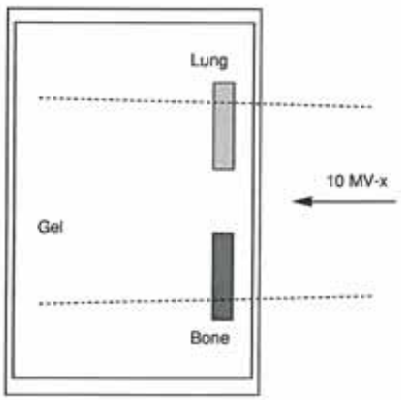

Fig. 6b Shematic presentation of the inhomogeneous phantom irradiation.

Fig. 7　Head phantom containing a human skull.

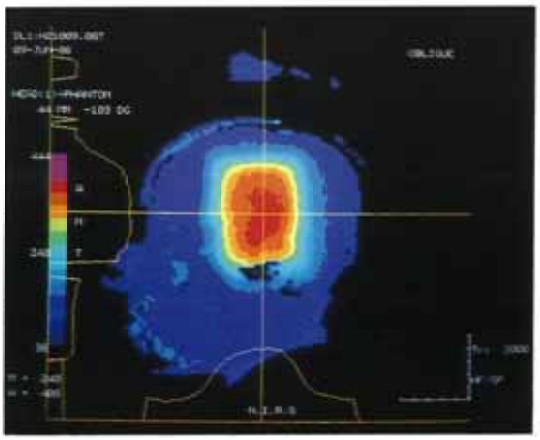

Fig. 9　Dose distribution image of the head phantom in a plane perpendicular to the beam axis.

Fig. 8　Thorax phantom.

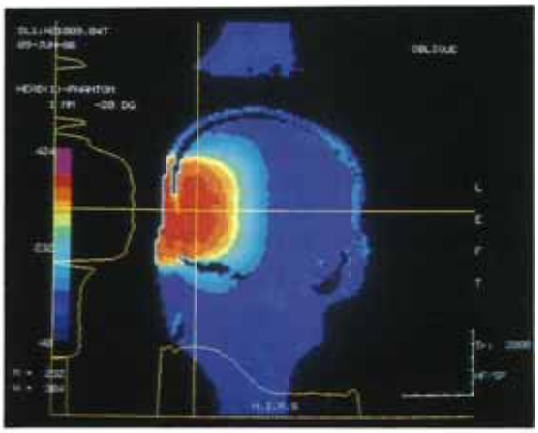

Fig. 10　Image of the head phantom in the coronal plane.

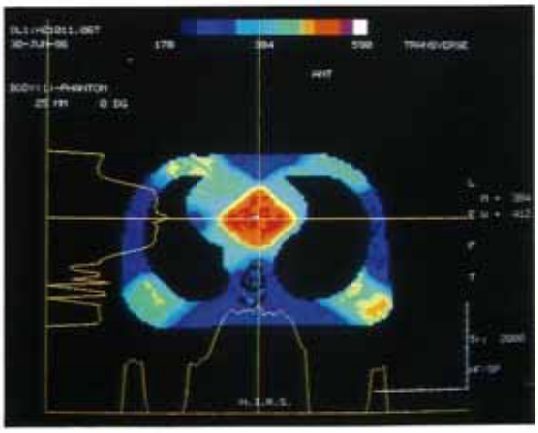

Fig. 11　Image of four oblique fields for treatment of the esophagus using the thorax phantom.

planning.

We attempted to make measurements of dose distributions in lung tissue. We made a lung gel phantom in which small styrofoam cubes were mixed with the gel (ρ=0.3 g/cm^3). The T_1 signal from the lung phantom was smaller than that from the gel phantom by the ratio of proton densities. We have found that the inversion recovery method of NMR will give a linear signal-to-dose ratio for dose D smaller than 25 Gy. We hope to combine the two methods to obtain images of the lung phantom, but so far we have not obtained satisfactory results.

Acknowledgments

The authors wish to thank Drs. H Bichsel, TA Iinuma and E Tanaka for their helpful advice. The authors also with to thank Mr. K Sakashita for his assistance in the phantom irradiations and Mr. T Takayama for making the body phantoms.

References

1) Gore JC, Kang VS, Schulz RJ: Measurement of radiation dose distributions by nuclear magnetic resonance (NMR) imager. Phys. Med. Biol. 29: 1189—1197, 1984
2) Hiraoka T, Fukuda N, Ikehira H et al: Digital imaging of dose distribution by magnetic resonance. Nippon Act. Radiol. 46: 503—505, 1986
3) Fricke U, Hart EJ: Chemical dosimetry. In Radiation Dosimetry, Vol II, ed, by Attix, Roesch and Tochilin, 167—239, 1966, Academic Press, New York
4) Radpath TW: Calibration of the Aberdeen NMR imager for proton spin-lattice relaxation time measurements in vitro. Phys. Med. Biol. 27: 1057—1065, 1982
5) White DR, Martin RJ, Darlison R: Epoxy resin based tissue substitutes. Br. J. Radiol. 50: 814—821, 1977